Circular Target Detection Method Based on Color Space Conversion and Morphological Filtering

Yixin Han
School of Computer Science and Engineering
Xi'an Technological University
Xi'an, China
E-mail: 1823338778@qq.com

***Abstract*—To address the low efficiency, high alignment error, and insufficient positioning reliability of single-sensor manual alignment in bulk cement truck loading, this paper proposes a circular target detection and localization method based on color space conversion, morphological filtering, and multi-sensor concurrent fusion. The proposed method first performs Gaussian preprocessing on industrial camera images to suppress high-frequency noise caused by dust, vibration, and illumination fluctuation. The filtered image is then converted from the RGB color space to the HSV color space, where calibrated dual red thresholds are used to obtain a binary mask of the circular port marker. Morphological erosion, dilation, opening, and closing are introduced to remove isolated noise, suppress edge burrs, and repair small discontinuities in the segmented region. On this basis, the FindContours algorithm extracts connected components, the largest valid contour is selected by geometric constraints, and minimum enclosing circle fitting is used to calculate the pixel center and radius of the target. To overcome the lack of absolute depth in monocular vision, an Arduino-based ultrasonic ranging module is further integrated, and a Python multiprocessing shared-memory mechanism is designed to decouple high-frame-rate image processing from low-baud-rate serial communication. Experimental results show that the proposed method effectively suppresses complex industrial background interference, outputs stable center coordinates, radius, and depth information, and accurately triggers the stop decision when the visual and ultrasonic thresholds are simultaneously satisfied, thereby improving the robustness and real-time performance of automated loading alignment.**

Keywords-Circular Target Detection; Hsv Threshold Segmentation; Morphological Filtering; Contour Extraction; Multi-Sensor Fusion

I. INTRODUCTION

With the rapid development of industrial automation and intelligent manufacturing, the intelligent operation of heavy-duty special vehicles has become an important part of improving production-flow efficiency. In bulk cement logistics and factory loading operations, precise alignment between the truck tank port and the factory feeding port is a prerequisite for automated filling. However, because cement trucks are large and the cab has severe visual blind zones, the traditional alignment process mainly depends on repeated manual parking adjustment and on-site guidance. This operating mode consumes labor and time, lowers logistics efficiency, and may cause material leakage, equipment collision, or loading-port damage when the alignment deviation is large.

Machine vision has been widely used in industrial inspection and target positioning because it provides non-contact measurements and rich scene information [1]-[3]. Nevertheless, visual perception in real factories is still affected by uneven illumination, dust, surface stains, local reflections, and complex background structures. Direct segmentation in the RGB color space is sensitive to brightness changes, and gradient-based edge detectors such as Canny may produce many false edges when the background contains scaffolding, concrete texture, or strong reflections [4], [15]. Therefore, a robust target perception method must combine illumination-tolerant color representation, noise filtering, and geometric verification.

Circular markers are common in industrial localization because their center and radius provide compact geometric features. Recent circular target studies show that the extraction quality of the image contour directly affects the stability of circle or ellipse fitting [5], [6]. For the cement loading scenario, the target is a specific colored circular port marker; therefore, the problem can be simplified into robust color segmentation and circular geometry fitting under interference. However, monocular vision alone provides only image-plane coordinates and a scale-related radius. It cannot directly provide reliable absolute distance. Multi-sensor fusion is thus necessary for complete spatial localization, and recent studies have demonstrated that fusing vision with ranging sensors can improve robustness and real-time positioning reliability [7]-[9].

To solve the above problems, this paper proposes a circular target detection method based on HSV color space conversion and morphological filtering and further designs a lightweight concurrent fusion architecture for camera and ultrasonic data. The main contributions are as follows. First, an HSV-threshold segmentation model is established to separate color and brightness information and to improve robustness against industrial illumination changes. Second, a morphology-contour-circle fitting pipeline is constructed to remove noise and obtain accurate target center and radius. Third, a multiprocessing shared-memory mechanism is introduced to synchronize visual output and ultrasonic distance without blocking, thereby supporting real-time alignment decisions.

II. RELATED WORK

Automated visual inspection has become one of the key technologies in manufacturing and maintenance. Recent surveys indicate that both traditional image processing and deep learning are used in industrial visual inspection, while real-time applications still often adopt rule-based image processing when the target color and geometry are known in advance [1], [3]. Benchmark studies also show that industrial scenes present diverse backgrounds, defects, and annotation requirements, which places higher demands on robust preprocessing and segmentation [2].

Color-space conversion is an effective solution for targets with stable chromatic features. Compared with RGB, HSV separates hue and saturation from the value channel, reducing the influence of brightness variation on color classification. In addition, common industrial preprocessing steps include Gaussian smoothing, threshold segmentation, morphology, connected-component analysis, and feature extraction [3], [10]. Morphological operations are particularly suitable for binary masks because they can emphasize object shapes, reduce isolated noise, fill small holes, and clarify object boundaries [3].

For circular target localization, Hough-based circle detection and ellipse/circle fitting are widely used. Lin et al. Improved Hough line and circle methods for real-time nut geometry inspection and demonstrated the value of geometry-constrained circle measurement in production-line inspection [4]. Hu et al. Proposed a space circular target detection method for machine vision and noted that circular target estimation is sensitive to contour and segmentation quality in practical imaging [5]. Maghami and Khoshdarregi further compared circular target localization methods for robotic pose correction, confirming that target localization accuracy directly affects downstream control performance [6].

Multi-sensor fusion is another key aspect of reliable localization. Barreto-Cubero et al. Fused stereo camera, LiDAR, and ultrasonic sensors for mobile robot perception, showing that different sensing modalities can complement each other [7]. Yang et al. Developed a two-stage multi-sensor positioning system for cooperative mobile robot and manipulator systems, combining ultrasonic, IMU, and visual positioning to enhance robustness [8]. Xu et al. Reviewed multi-sensor fusion SLAM and pointed out that single-sensor systems are prone to degradation in complex scenes [9]. These studies motivate the fusion of image-plane circular target detection with ultrasonic absolute depth for cement-truck loading alignment.

III. PROPOSED TARGET DETECTION METHOD

A. Overall Architecture of the Algorithm

The proposed system contains six closely connected steps: image preprocessing, HSV threshold segmentation, morphological filtering, contour extraction, circle fitting, and multi-sensor concurrent localization. The industrial camera continuously captures RGB images, while the ultrasonic module provides the longitudinal distance. The visual process outputs the target center (u_c, v_c) and pixel radius, and the serial process outputs the ultrasonic distance Z. The main process reads these data from sharedmemory and generates the final alignment decision.

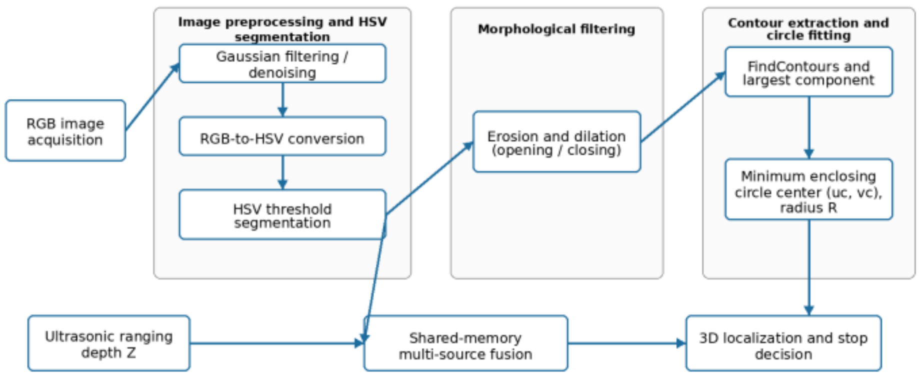

Figure 1. Overall flowchart of the proposed target detection and multi-sensor localization algorithm

B. Image Preprocessing and HSV Threshold Segmentation

Let the input image acquired by the industrial camera be $I_{RGB}(x,y)$. Dust, vibration, sensor noise, and illumination fluctuation introduce high-frequency components. Gaussian filtering is applied before segmentation:

$$(x,y)=\frac{1}{2\pi\sigma^2}\exp\left[-\frac{x^2+y^2}{2\sigma^2}\right], I_g = G*I_{RGB}. \quad (1)$$

Where (x,y) is the pixel coordinate, * is the standard deviation, * denotes convolution, and I_g is the denoised image. A 5×5 kernel is used in the experiment to balance noise suppression and edge preservation.

After denoising, the image is converted into the HSV color space. For normalized RGB components R', G', and B', define $C_{\max} = \max(R',G',B')$, $C_{\min} = \min(R',G',B')$, and $\Delta = C_{\max} - C_{\min}$. The value and saturation channels are expressed as

$$S=\begin{cases}0, & C_{\max}=0,\\ \dfrac{\Delta}{C_{\max}}, & C_{\max}\neq 0.\end{cases} \quad V = C_{\max} \quad (2)$$

The hue channel is calculated by

$$H=\begin{cases}60^\circ\left[\dfrac{G'-B'}{\Delta}\bmod 6\right], & C_{\max}=R',\\ 60^\circ\left(\dfrac{B'-R'}{\Delta}+2\right), & C_{\max}=G',\\ 60^\circ\left(\dfrac{R'-G'}{\Delta}+4\right), & C_{\max}=B'.\end{cases} \quad (3)$$

Because the target marker is red, its hue interval crosses the circular boundary of the hue axis. Therefore, a dual-threshold strategy is used. Let $\mathbf{P}(x,y)=[\mathbf{H}(x,y),\mathbf{S}(x,y),\mathbf{V}(x,y)]^{\mathrm{T}}$, $\Omega_r = \Omega_1 \cup \Omega_2$, $\Omega_1 = [0,43,46]\sim[10,255,255]$, and $\Omega_2 = [156,43,46]\sim[180,255,255]$. The binary mask is

$$M_0(x,y)=\begin{cases}1, & P(x,y)\in\Omega_r,\\ 0, & \text{otherwise.}\end{cases} \tag{4}$$

This operation is equivalent to OpenCV's inRange thresholding. It extracts the target chromatic region while suppressing most background pixels.

C. Morphological Filtering

Although HSV segmentation separates the target color, the initial binary mask may contain isolated white noise, edge burrs, and holes. Let A denote the foreground set of M_0 , and let B denote the structuring element. Erosion removes foreground regions smaller than the structuring element:

$$A\bullet B=\left(A\oplus B\right)!\ \ B; \tag{5}$$

Dilation expands the foreground and reconnects local discontinuities:

$$A\oplus B=\left\{z\bar{o}\,\hat{B}_z\cap A\neq\varnothing\right\} \tag{6}$$

Where B_z is the translation of B by z , and $\hat{B}$ is the reflection of B. The opening and closing operations are defined as

$$A\bullet B=\left(A\oplus B\right)!\ \ B\ \ !A^{\circ}B=\left(A!\ \ B\right)\oplus B \tag{7}$$

In the proposed algorithm, the opening operation removes isolated noise and small burrs, while the closing operation fills small holes and restores edge continuity. The resulting mask is denoted as Mc.

D. Contour Extraction and Circular Geometric Fitting

After obtaining $\mathbf{M}_c$, the find contours algorithm is used to extract all external connected-component contours $\mathrm{C}=\left\{C_1,C_2,\ldots,C_n\right\}$. The area of the i the contour is

$$S_i=\frac{1}{2}\left|\sum_{k=1}^{m_i}\left(x_k y_{k+1}-x_{k+1}y_k\right)\right|. \tag{8}$$

Because the target marker occupies the main field of view during alignment, the largest connected component satisfying the area constraint is selected:

$$C^*=\underset{C_i\in\mathrm{C}}{\operatorname{argmax}}\,S_i,\quad S_i>S_{\min}. \tag{9}$$

For the point set $p_k=\left(x_k,y_k\right)\in C^*$, minimum enclosing circle fitting estimates the center $c=\left(u_c,v_c\right)$ and radius R by solving.

$$\min_{c,R}R,\quad \text{s.t.}\left\|p_k-c\right\|_2\le R, k=1,2,\ldots,m. \tag{10}$$

The fitting result converts the segmented target region into compact image-plane localization parameters. When camera intrinsic parameters are available, the center can be further normalized as

$$x_n=\frac{u_c-c_x}{f_x},\quad y_n=\frac{v_c-c_y}{f_y}. \tag{11}$$

Where $\left(f_x,f_y\right)$ are focal lengths and $\left(c_x,c_y\right)$ is the principal point.

E. Multi-Sensor Concurrent Localization

Monocular vision provides accurate image-plane coordinates but cannot directly output absolute depth. Therefore, an HC-SR04 ultrasonic sensor is introduced. If the trigger-to-echo time is Δt and the sound velocity is Vs, the longitudinal distance is:

$$Z=\frac{v_s\Delta t}{2}. \tag{12}$$

The visual process and the serial process have different update frequencies. To prevent blocking, a Python multiprocessing structure with shared memory is designed. The shared state vector is:

$$x_s(t)=[u_c(t), v_c(t), R(t), Z(t), \tau(t)]^T \quad (13)$$

Where $\tau(t)$ is the timestamp. The visual process updates (u_c, v_c, R), the serial process updates Z, and the main process reads $s(t)$ using a lock-protected shared-memory manager. The final alignment command is determined by a binary decision variable:

$$D(t)=\begin{cases}1, & R(t)\geq R_{\text{th}} \wedge Z(t)\leq Z_{\text{th}},\\ 0, & \text{otherwise.}\end{cases} \quad (14)$$

Where $D(t)=1$ denotes the stop command and $D(t)=0$ denotes the approaching state. In this study, $R_{\text{th}}=180$ px and $Z_{\text{th}}=30$ cm. The logical AND condition prevents premature stopping when only the lateral or longitudinal criterion is satisfied.

IV. Experiments and Result Analysis

A. Experimental Platform and Parameter Settings

A prototype verification platform was established to evaluate the proposed method. The host computer executed the visual algorithm in Python 3.13.0 using the OpenCV library. An industrial camera captured RGB images, while an Arduino Uno and an HC-SR04 ultrasonic ranging module provided depth data through serial communication.

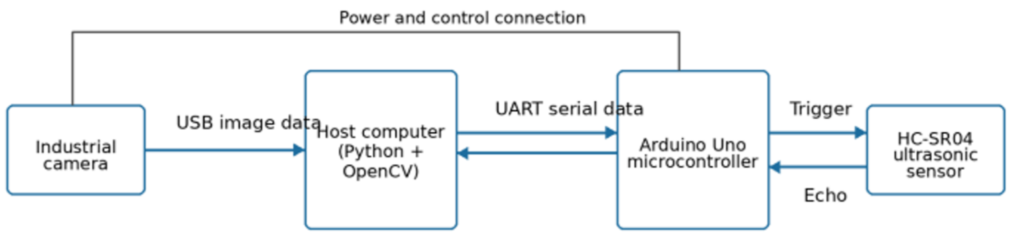

Figure 2. Hardware architecture topology of the experimental platform.

TABLE I. HARDWARE AND ALGORITHM PARAMETERS

Item	Setting
Development language	Python 3.13.0
Vision library	OpenCV
Camera input	RGB industrial camera
Gaussian kernel	5 × 5
HSV threshold 1	[0,43,46] to [10,255,255]
HSV threshold 2	[156,43,46] to [180,255,255]
Morphological kernel	3 × 3, two iterations
Ranging module	HC-SR04 ultrasonic sensor
Serial baud rate	9600 bps
Stop thresholds	R >= 180 px and Z <= 30 cm

B. Verification of the Visual Target Detection Algorithm

To evaluate robustness against complex backgrounds, target recognition tests were conducted in a simulated industrial environment. The original RGB image was first smoothed and converted into the HSV color space. The dual red threshold generated an initial mask, but the mask still contained discrete noise and small edge burrs. After morphological filtering, isolated noise points were removed, holes were repaired, and the target region became smooth and connected. The final contour was extracted and fitted with a circle, producing the target center and radius in real time.

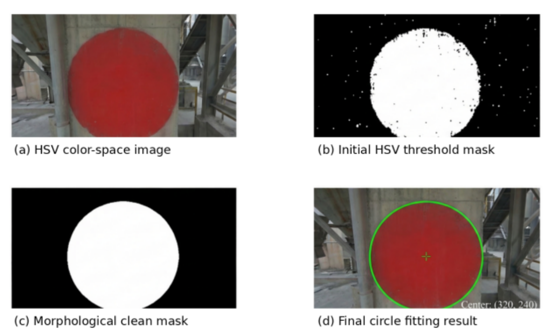

Figure 3. Stage-by-stage processing results of the proposed visual algorithm: (a) HSV color-space image; (b) initial HSV threshold mask; (c) morphological clean mask; (d) final circle fitting result.

C. Comparative Experiment with Traditional Edge Detection

The traditional Canny edge detector was used as a comparison method under the same lighting and background conditions. As shown in Figure 4, Canny can extract gradient changes, but the extracted edges are severely fragmented in the presence of surface stains, reflection, and background texture. Many irrelevant structural lines are also detected, which makes it difficult to obtain a stable circular contour. In contrast, the proposed method first isolates the target color in HSV space and then repairs the mask by morphology. The resulting circular contour is continuous and clean, which improves the reliability of center and radius estimation.

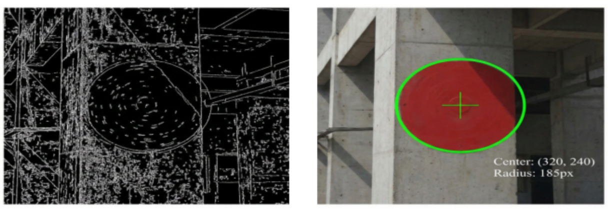

(a) Traditional Canny edge detection (b) Proposed HSV-morphology method

Figure 4. Detection performance comparison under complex lighting: (a) traditional Canny edge detection; (b) proposed HSV-morphology method.

D. *Multi-Source Fusion Localization and Performance Analysis*

The real-time output interface is shown in Figure 5. When the visual radius and ultrasonic distance simultaneously satisfy the thresholds, the system outputs the stop command. Otherwise, it continues to indicate the approaching state. The shared-memory architecture decouples the high-frequency visual loop from the low-frequency serial loop and avoids frame lag caused by serial blocking.

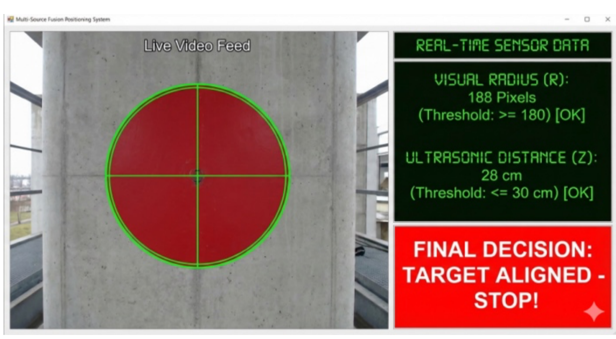

Figure 5. Real-time output interface of the multi-source fusion positioning system.

Ten dynamic alignment trials were conducted. The actual physical distance, ultrasonic feedback, visual radius, and system decision were recorded. The performance summary is listed in Table II.

TABLE II. POSITIONING PERFORMANCE SUMMARY

Metric	Value
Number of trials	10
Distance range	25.0-52.0 cm
Maximum ultrasonic error	1.7 cm
Stop threshold	R >= 180 px and Z <= 30 cm
False or missed stop	0
Stop decision accuracy	100%

The ultrasonic error remains within 1.7 cm in the tested range, and the visual radius increases consistently as the vehicle approaches the target. In all ten trials, the stop command was triggered only when both the lateral visual criterion and the longitudinal distance criterion were satisfied. No false stop or missed stop occurred in the experiment, demonstrating that the proposed fusion strategy provides reliable decision support for automated loading alignment.

V. CONCLUSIONS

This paper proposed a circular target detection and localization method based on HSV color space conversion, morphological filtering, contour extraction, circle fitting, and multi-sensor concurrent fusion. The method first uses Gaussian filtering to suppress image noise and HSV dual-threshold segmentation to extract the red circular marker. Morphological opening and closing then remove isolated noise and repair local mask defects. The FindContours algorithm and minimum enclosing circle fitting are used to calculate the target center and radius. Finally, ultrasonic ranging and multiprocessing shared memory are introduced to obtain absolute depth and avoid blocking between image processing and serial communication.

The experimental results show that the proposed method can robustly detect the circular target under complex industrial background interference and can combine visual and ultrasonic information to output stable alignment decisions. Future work will focus on three aspects: integrating lightweight deep learning detectors to improve robustness under extreme dust or illumination conditions, porting the algorithm to embedded edge platforms such as Raspberry Pi or NVIDIA Jetson, and introducing temporal tracking and closed-loop vehicle control to realize fully automated parking alignment.

REFERENCES

[1] N. Huetten, M. A. Gomes, F. Hoelken, K. Andricevic, R. Meyes, and T. Meisen, "Deep learning for automated visual inspection in manufacturing and maintenance: A survey of open-access papers," Applied System Innovation, vol. 7, no. 1, Art. no. 11, 2024, doi: 10.3390/asi7010011.

[2] H. Bai, S. Mou, T. Likhomanenko, R. G. Cinbis, O. Tuzel, P. Huang, J. Shan, and M. Cao, "VISION datasets: A benchmark for vision-based industrial inspection," arXiv:2306.07890, 2023.

[3] A. Ercetin, O. Der, F. Akkoyun, M. P. G. Chandrashekarappa, R. Sener, M. Calisan, N. Olgun, G. Chate, and K. N. Bharath, "Review of image processing methods for surface and tool condition assessments in machining," Journal of Manufacturing and Materials Processing, vol. 8, no. 6, Art. no. 244, 2024, doi: 10.3390/jmmp8060244.

[4] E.-Y. Lin, C.-T. Tu, and J.-J. J. Lien, "Nut geometry inspection using improved Hough line and circle methods," Sensors, vol. 23, no. 8, Art. no. 3961, 2023, doi: 10.3390/s23083961.

[5] W. Hu, J. Chi, J. Liu, and Z. Yang, "A novel method for space circular target detection in machine vision," Sensors, vol. 22, no. 3, Art. no. 769, 2022, doi: 10.3390/s22030769.

[6] A. Maghami and M. Khoshdarregi, "Vision-based target localization and online error correction for high-precision robotic drilling," Robotica, vol. 42, no. 9, pp. 3019-3043, 2024, doi: 10.1017/S0263574724001255.

[7] A. J. Barreto-Cubero, A. Gomez-Espinosa, J. A. Escobedo Cabello, E. Cuan-Urquizo, and S. R. Cruz-Ramirez, "Sensor data fusion for a mobile robot using neural networks," Sensors, vol. 22, no. 1, Art. no. 305, 2022, doi: 10.3390/s22010305.

[8] M. Yang, G. Li, and Y. Wang, "Two-stage multi-sensor fusion positioning system with seamless switching for cooperative mobile robot and manipulator system," International Journal of Intelligent Robotics and Applications, vol. 7, pp. 283-300, 2023, doi: 10.1007/s41315-023-00276-0.

[9] X. Xu, L. Zhang, J. Yang, C. Cao, W. Wang, Y. Ran, Z. Tan, and M. Luo, "A review of multi-sensor fusion SLAM systems based on 3D LiDAR," Remote Sensing, vol. 14, no. 12, Art. no. 2835, 2022, doi: 10.3390/rs14122835.

[10] R.-Q. Qiu, "Integrated automatic optical inspection and image processing method for PCB welding spot detection," Sensors, vol. 24, no. 5, Art. no. 1619, 2024, doi: 10.3390/s24051619.

[11] S. Lee, J. Kim, and H. Park, "Defect recognition and morphology operation in binary images," Applied Sciences, vol. 12, no. 12, Art. no. 6006, 2022.

[12] G. Bradski and A. Kaehler, Learning OpenCV 3: Computer Vision in C++ with the OpenCV Library. Sebastopol, CA, USA: O'Reilly Media, 2016.

[13] R. C. Gonzalez and R. E. Woods, Digital Image Processing, 4th ed. New York, NY, USA: Pearson, 2018.

[14] S. Suzuki and K. Abe, "Topological structural analysis of digitized binary images by border following," Computer Vision, Graphics, and Image Processing, vol. 30, no. 1, pp. 32-46, 1985, doi: 10.1016/0734-189X(85)90016-7.

[15] J. Canny, "A computational approach to edge detection," IEEE Transactions on Pattern Analysis and Machine Intelligence, vol. PAMI-8, no. 6, pp. 679-698, 1986, doi: 10.1109/TPAMI.1986.4767851.